



**HAL**  
open science

## **Engraftment of chronic myelomonocytic leukemia cells in immunocompromised mice supports disease dependency on cytokines**

Yanyan Zhang, Liang He, Dorothée Selimoglu-Buet, Chloe Jegu, Margot Morabito, Christophe Willekens, M'Boyba Khadija Diop, Patrick Gonin, Valérie Lapierre, Nathalie Droin, et al.

### ► **To cite this version:**

Yanyan Zhang, Liang He, Dorothée Selimoglu-Buet, Chloe Jegu, Margot Morabito, et al.. Engraftment of chronic myelomonocytic leukemia cells in immunocompromised mice supports disease dependency on cytokines. *Blood Advances*, 2017, 1 (14), pp.972-979. 10.1182/bloodadvances.2017004903 . hal-04438691

**HAL Id: hal-04438691**

**<https://hal.science/hal-04438691>**

Submitted on 4 Sep 2024

**HAL** is a multi-disciplinary open access archive for the deposit and dissemination of scientific research documents, whether they are published or not. The documents may come from teaching and research institutions in France or abroad, or from public or private research centers.

L'archive ouverte pluridisciplinaire **HAL**, est destinée au dépôt et à la diffusion de documents scientifiques de niveau recherche, publiés ou non, émanant des établissements d'enseignement et de recherche français ou étrangers, des laboratoires publics ou privés.

# Engraftment of chronic myelomonocytic leukemia cells in immunocompromised mice supports disease dependency on cytokines

Yanyan Zhang,<sup>1,2</sup> Liang He,<sup>1,2</sup> Dorothée Selimoglu-Buet,<sup>1,2</sup> Chloe Jego,<sup>1,2</sup> Margot Morabito,<sup>1,2</sup> Christophe Willekens,<sup>3</sup> M'boyba Khadija Diop,<sup>1,2</sup> Patrick Gonin,<sup>4</sup> Valérie Lapierre,<sup>5</sup> Nathalie Droin,<sup>1,2</sup> Eric Solary,<sup>1,2,6</sup> and Fawzia Louache<sup>1,2,7</sup>

<sup>1</sup>INSERM U1170, Gustave Roussy, Villejuif, France; <sup>2</sup>Université Paris-Sud, Orsay, France; <sup>3</sup>Department of Clinical Hematology, Gustave Roussy, Villejuif, France; <sup>4</sup>INSERM US23/Centre National de la Recherche Scientifique UMS3655, Analyse Moléculaire, Modélisation et Imagerie de la maladie cancéreuse, Gustave Roussy, Villejuif, France; <sup>5</sup>Centre de Thérapie cellulaire, Gustave Roussy, Villejuif, France; <sup>6</sup>Faculté de Médecine Paris-Sud, Le Kremlin-Bicêtre, France; and <sup>7</sup>Centre National de la Recherche Scientifique Groupement De Recherche 3697 MicroNIT, Villejuif, France

## Key Points

- Transgenic mice expressing 3 human cytokines enable expansion of CMML cells with limited stem cell engraftment.
- The mutational profile of CMML cells that expand in mice mirrors that of patient monocytes.

Chronic myelomonocytic leukemia (CMML) is a clonal hematopoietic stem cell disorder that typically associates with mutations in epigenetic, splicing, and signaling genes. Genetically modified mouse models only partially recapitulate the disease phenotype, whereas xenotransplantation of CMML cells in immunocompromised mice has been rarely successful so far. Here, CMML CD34<sup>+</sup> cells sorted from patient bone marrow (BM) or peripheral blood (PB) were injected intravenously into NSG (NOD/LtSz-scid IL2r $\gamma$ null) mice and NSG mice engineered to express human granulo-monocyte colony-stimulating factor, stem cell factor, and interleukin-3 (NSGS mice). Fifteen out of 16 patient samples (94%) successfully engrafted into NSG or NSGS or both mouse strains. The expansion of human cells, predominant in the BM, was also observed in the spleen and the PB and was greatly enhanced in mice producing the 3 human cytokines. Gene mutations identified in engrafted cells were mostly similar to those identified in patient cells before injection. Successful secondary engraftment was obtained in NSGS mice in 3 out of 10 attempts. Thus, primary CMML leukemic cells expand much better in NSGS compared with NSG mice with limited efficacy of secondary transplant.

## Introduction

Chronic myelomonocytic leukemia (CMML), the most frequent myelodysplastic/ myeloproliferative neoplasm, is defined by a persistent peripheral blood (PB) monocyte count higher than  $1 \times 10^9/L$ .<sup>1</sup> Genomic analyses identified a mean number of 14 somatic mutations in the coding regions of DNA and mutational signatures of aging.<sup>2</sup> Typically, the disease involves a combination of mutations in epigenetic genes, mostly *TET2* (ten eleven translocation-2) and *ASXL1* (additional sex combs like 1), splicing genes, mostly *SRSF2* (serine/arginine-rich splicing factor 2), and signaling genes of the Ras pathway.<sup>2,3</sup> A key feature of CMML is the enhanced sensitivity of a CD38-expressing progenitor population to granulocyte-macrophage colony-stimulating factor (GM-CSF). GM-CSF neutralization was therefore proposed as a potential therapeutic strategy in this difficult-to-treat disease.<sup>4,5</sup> Genetically modified mouse models only partially recapitulate the phenotypic heterogeneity of CMML.<sup>6</sup> An alternative approach is the xenotransplantation of human diseased cells in immunocompromised mice. In a previous series, only 4 out of 8 CMML samples engrafted in nonobese diabetic, severe combined immunodeficiency (NOD-SCID) mice, pending the transgenic expression of human GM-CSF in recipient animals.<sup>7</sup> In this previous study, the general strategy was to inject total bone marrow (BM) or PB without CD34-based immunoselection, making it difficult to draw conclusions about the potential of CMML-derived stem cells to engraft and differentiate in immunodeficient mice. Thus, the question remains as to whether

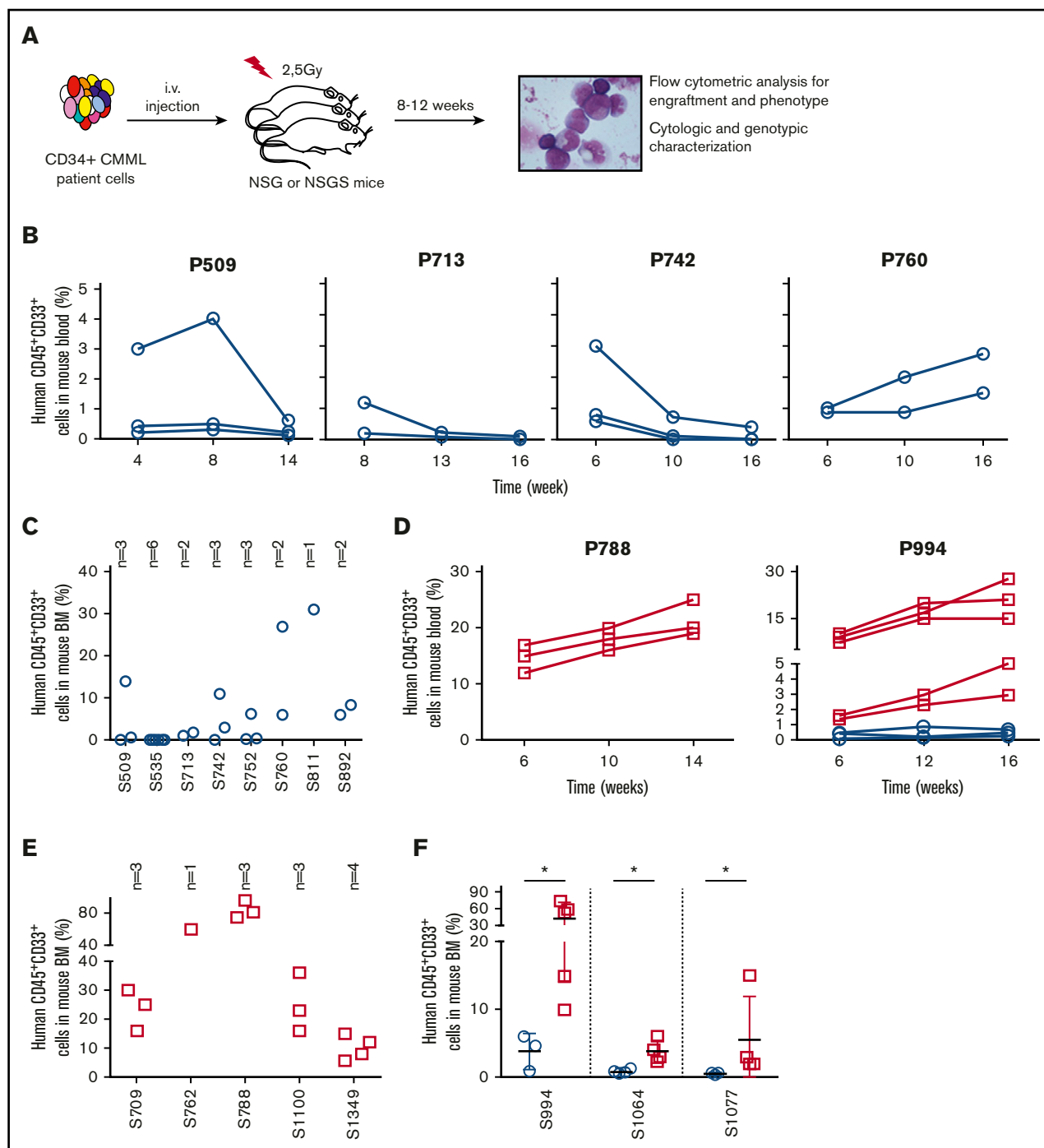


**Figure 1. Engraftment of CMML CD34<sup>+</sup> cells in NSG and NSGS mice.** (A) General experimental procedure for engraftment. CD34<sup>+</sup> cells were sorted from PB or BM samples collected from CMML patients using the MACS system (Miltenyi Biotec). One to 6 female mice, 6 to 8 weeks old, were irradiated at 2.5 Gy with a radiograph irradiator and IV injected within 24 hours with CD34<sup>+</sup> cells suspended in 200  $\mu$ L PBS. Human CD45<sup>+</sup>CD33<sup>+</sup> cells were identified by flow cytometry in mouse blood samples collected at indicated time points postengraftment into NSG (B) or NSGS (D, left) or both (D, right) mice and in mouse BM samples taken from NSG (C) or NSGS (E) or both (F) mice when euthanized, 12 to 16 weeks after transplantation of cells from indicated samples. Each circle/square represents an individual mouse. "S" indicates the sample number. NSG mice are indicated by empty blue circles and NSGS mice by empty red squares.

CMML CD34<sup>+</sup> stem cells may engraft in immunodeficient mice. Since this report, new immunodeficient strains have been established through disruption of the interleukin-2 (IL-2) receptor common  $\gamma$ -chain (IL2R $\gamma$ null), including NOD/Shi-Scid IL2 $\gamma$ null (NOG), NOD/LtSz-scid

IL2 $\gamma$ null (NSG), and BALB/c Rag2nullIL2 $\gamma$ null, enabling long-term engraftment of human tissues.<sup>8</sup> Some of these strains were further engineered to express human stem cell factor (SCF), GM-CSF, and IL-3 to generate the SGM3-Tg model or NSGS.<sup>9</sup> Immunodeficient Rag2<sup>-/-</sup>

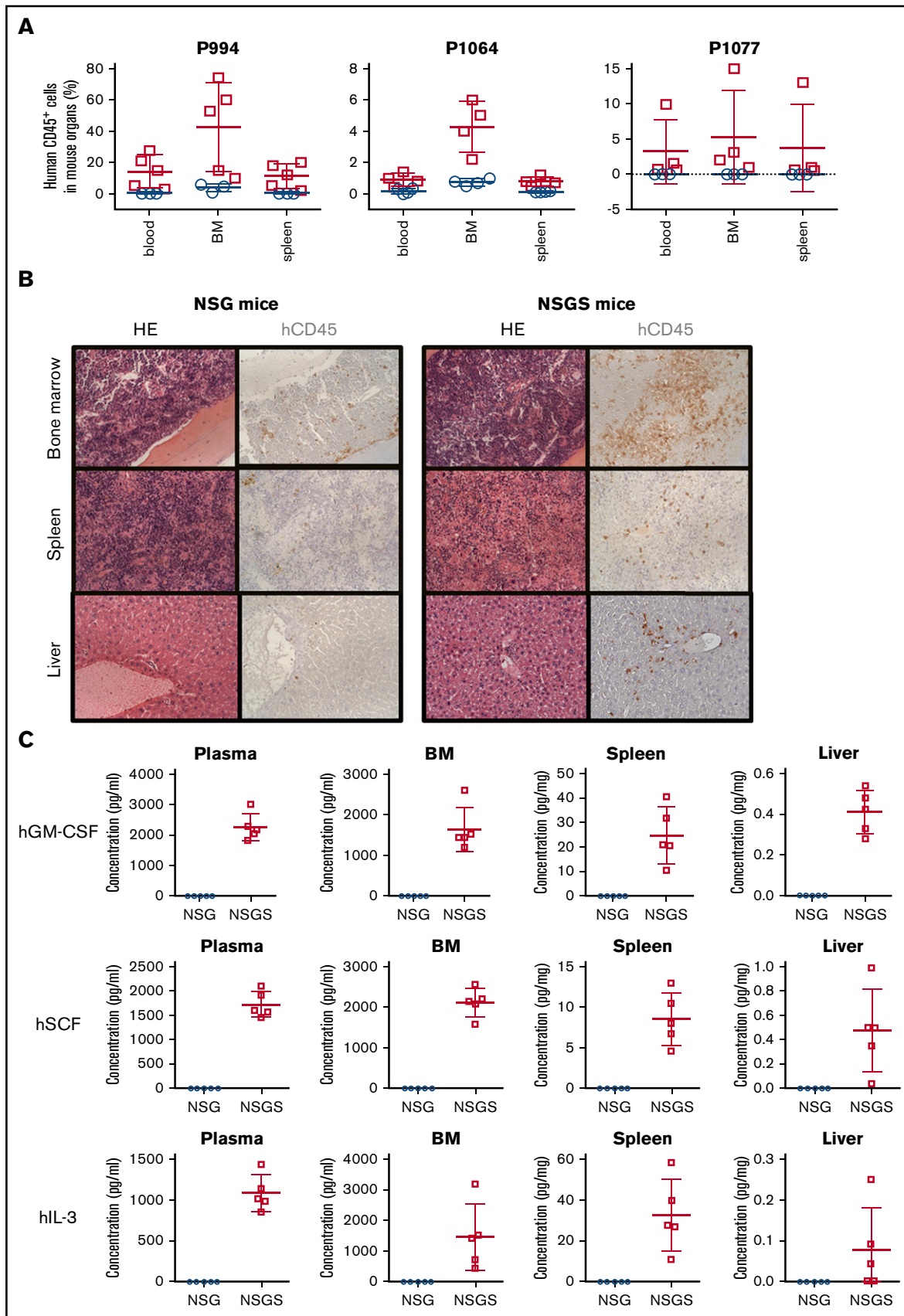


Figure 2.

*Il2ry*<sup>-/-</sup> mice were also engineered to express human macrophage colony-stimulating factor, IL-3, GM-CSF, and thrombopoietin or signal regulatory protein  $\alpha$  (MITRG [CSF1/IL3/CSF2/TPO/Rag2<sup>-/-</sup>Il2rg<sup>-/-</sup>] and MISTRG [CSF1/IL3/CSF2/SIRPA/TPO/Rag2<sup>-/-</sup>Il2rg<sup>-/-</sup>] mice), allowing engraftment of acute myeloid leukemia samples reported to be nontransplantable in nonengineered strains.<sup>10-12</sup> Here, we show for the first time that CD34<sup>+</sup> CMML cells engraft more efficiently in NSGS compared with NSG mice. Using immunophenotypical markers, we demonstrate that injected CD34<sup>+</sup> cells differentiate in mice. In addition, we show that secondary transplantation is possible, at least for some CMML cases. Finally, we provide evidence that xenotransplantation preserves the molecular characteristics of the primary disease.

## Materials and methods

### Patients and samples

BM (n = 6) or PB (n = 10) were collected from CMML patients at diagnosis after informed consent and following protocols approved by local Research Ethics Committees from Gustave Roussy (Villejuif, France) and Saint Antoine Hospital (Paris, France). The diagnosis of CMML was established according to World Health Organization classification criteria. Cytogenetic risk was classified according to the Spanish CMML classification.<sup>13,14</sup> Gene mutations were screened as described previously. Details of the patient samples are listed in supplemental Table 1. Mononuclear cells were obtained by Ficoll-Paque density centrifugation before CD34<sup>+</sup> cell sorting using the MACS system (Miltenyi Biotec, Auburn, CA).

### Mice and xenogeneic transplantation

NSG mice and NSGS mice were purchased from the Jackson Laboratory and were bred and maintained under specific pathogen-free conditions at the animal facility of Gustave Roussy. Mice were aged 6 to 8 weeks at the start of the experiment with a weight of 20 to 26 g. Animal experiments were conducted in accordance with institutional and national guidelines and approved by the Ethical Committee C2EA-26. Mice were sublethally irradiated at 2.5 Gy with an radiograph irradiator. Twenty-four hours after irradiation, hCD34<sup>+</sup> cells ( $3 \times 10^4$  to  $1.2 \times 10^6$  per animal) were injected in 200  $\mu$ L phosphate-buffered saline (PBS) via the retro-orbital venous sinus under isoflurane gas anesthesia. Bleeding was performed every 4 to 6 weeks, and mice were euthanized at 10 to 16 weeks posttransplantation by cervical dislocation under isoflurane gas anesthesia.

### Assessment of engraftment

At different weeks postengraftment, blood was taken from the retro-orbital sinus of anesthetized mice to analyze the reconstitution by human cells as described previously.<sup>15</sup> Mice were euthanized at 10 to 16 weeks postengraftment. Cells from blood, BM, and spleen were stained with the following monoclonal antibodies: allophycocyanin (APC)/Cy7 conjugated rat anti-mouse CD45 (Beckman Coulter), phycoerythrin (PE)/Cy7-conjugated mouse anti-human CD45, human specific PE-conjugated anti-CD19, PerCP/Cy5.5-conjugated

anti-CD33, Pacific blue-conjugated anti-CD14, Pacific orange-conjugated anti-CD15, APC-conjugated anti-CD34 and fluorescein isothiocyanate-conjugated anti-CD3 (all from BD Pharmingen). Stained cells were analyzed on a FACScanto II cytometry (BD Biosciences).

### Secondary transplantation

For secondary transplantation, the cellular content of 2 femurs and 2 tibias was flushed in 1 mL PBS. Human cells were isolated by EasySep Mouse/Human Chimera Isolation Kit (Stemcell Technologies Inc.). Isolated human cells were suspended in 200  $\mu$ L PBS and IV injected into irradiated mice. Human cells engraftment was assessed 8 to 16 weeks later.

### Histopathology and immunohistochemistry

Femur, spleen, and liver samples were fixed overnight in FineFix (Milestone), dehydrated, and paraffin embedded, and sections (4  $\mu$ m thick) were prepared. After hematoxylin-eosin-safranin staining was performed on all of the samples, sections were examined. For immunohistochemical labeling, sections were deparaffinized and rehydrated. For CD45 immunohistochemistry, paraffin sections were processed for heat-induced antigen retrieval in 10 mM citrate buffer (pH 7.3) and incubated with a mouse anti-human CD45 monoclonal antibody (1:200; Dako, Trappes, France) for 60 minutes. Staining was visualized by Histomouse Kit (Zymed). Finally, the sections were counterstained with hematoxylin. All slides were immunostained in cover plates the same day, guaranteeing a standardized intensity of staining. Each slide was examined using a Zeiss Axiophot microscope.

### Targeted next-generation sequencing

Human cells were sorted from BM of engrafted mice using the EasySep Mouse/Human Chimera Isolation Kit (Stemcell Technologies Inc.) with a purity of human cells >90%. DNA was extracted from patient material or human cells sorted using QIAamp DNABlood Mini Kit (Qiagen) and quantified using the Qubit dsDNA HS Assay Kit (Thermo Fisher Scientific), according to the manufacturer's instructions. Samples were sequenced on the Illumina MiSeq platform using Ion AmpliSeq Custom Myeloid Panel Primer Pools (10 ng of genomic DNA per primer pool) to perform multiplex polymerase chain reaction. Libraries were generated with addition of paired-end adaptors (NEXTflex; Bioo Scientific) before paired-end sequencing (2  $\times$  150 bp reads) using an Illumina MiSeq flow cell and the onboard cluster method (Illumina, San Diego, CA). Quality of reads was evaluated using FastQC. For each sample, paired read sequences (150 bp each) were obtained and mapped to hg19 and mm10 reference genome sequences, to take into account murine DNA contamination.

### Cytokine analysis

Citrated blood was obtained from the retro-orbital sinus, and plasma was prepared. The BM content of 2 femurs was flushed in

**Figure 2. Characterization of cells that engrafted in NSG and NSGS mice.** (A) The fraction of human CD45<sup>+</sup> (hCD45<sup>+</sup>) cells was measured by flow cytometry in blood, BM, and spleen of NSG (empty blue circles) and NSGS (empty red squares) mice engrafted with indicated CMML samples and euthanized 12 to 16 weeks after transplantation. (B) Hematoxylin and eosin (HE) staining and immunohistochemical analysis of hCD45<sup>+</sup> cells on the BM, spleen, and liver of NSG (left panels) or NSGS (right panels) mice engrafted with CMML CD34<sup>+</sup> cells sorted from S994. Original magnification  $\times$ 200. (C) Concentration of human GM-CSF (hGM-CSF), SCF (hSCF), and IL-3 (hIL-3) detected in the plasma, BM, spleen, and liver of NSG (empty blue circles) and NSGS (empty red squares) mice.

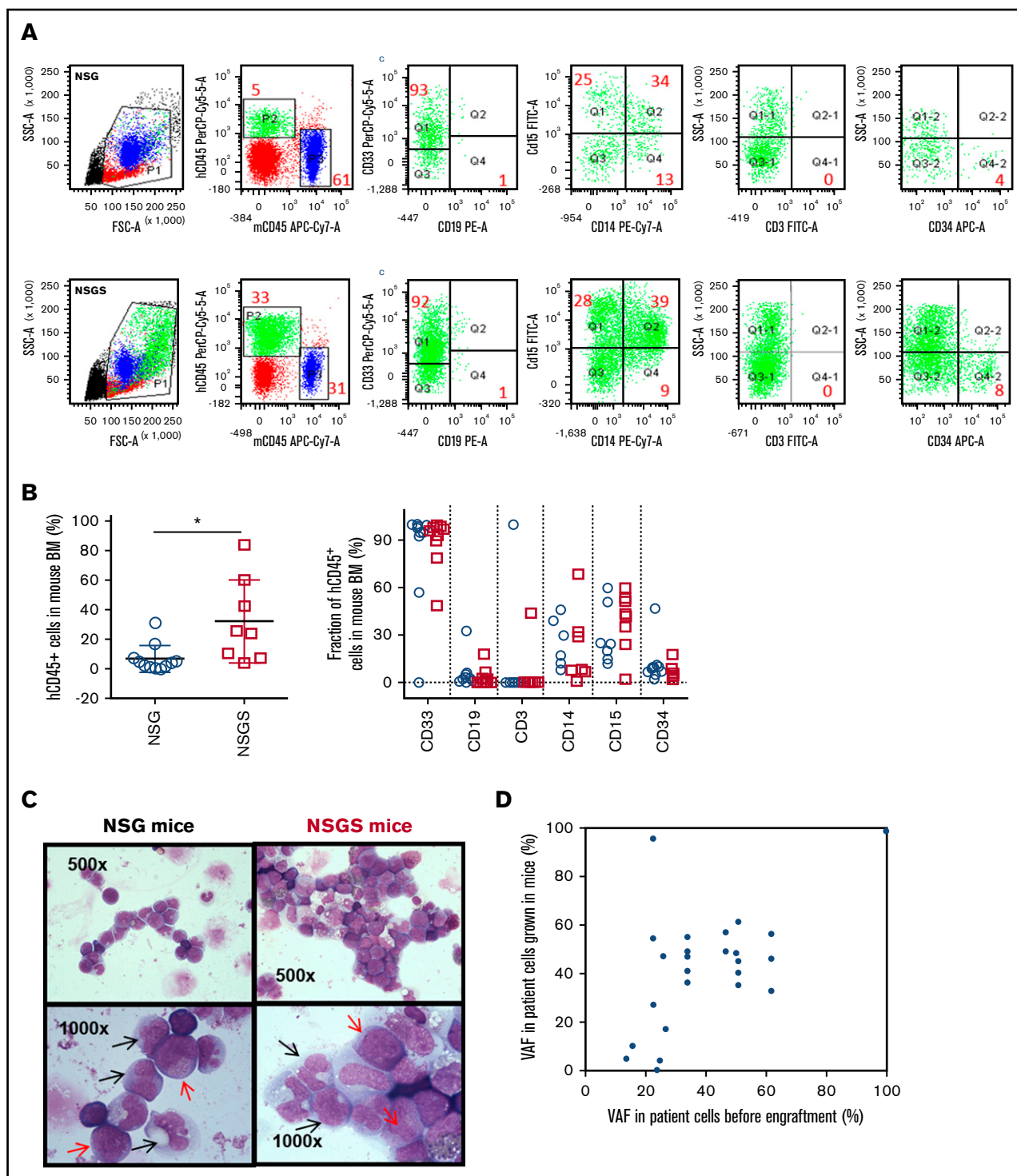


**Figure 3. Multiparameter flow cytometry analysis of hCD45<sup>+</sup> cells in the BM of engrafted mice.** (A) Representative dot plot of flow cytometry analysis for immunophenotype of BM from NSG and NSGS mice xenografted from S944. The numbers listed represent the percent of human cells within gates P1 and P2 shown in left panel. (B) Percentage of human hCD45<sup>+</sup> cells (left) within gates P1 and P2 calculated from NSG (11 patients) and NSGS (8 patients) primary mice 12 to 16 weeks posttransplantation. Each circle/square represents the mean percentage of human cells in different mice reconstituted with the same patient. Indicated fraction of cells among hCD45<sup>+</sup> cells (right panel) in BM samples collected. No statistical differences were found in the percentages of cells expressing the different markers including CD34, CD15, and CD14 (Mann-Whitney *U* test). (C) Cytomorphology of human cells sorted from BM of NSG (left panels) and NSGS (right panels) recipient mouse xenografted from patient (S994). Black arrows indicate promonocytes and monoblasts; red arrows indicate myeloblasts. Original magnification  $\times 500$  (top panels) and  $\times 1000$  (bottom panels). (D) Genetic variants whose allele frequency (VAF) was measured in patient cells before and after engraftment in an NSGS mouse. Each dot represents 1 given mutation among screened genes.

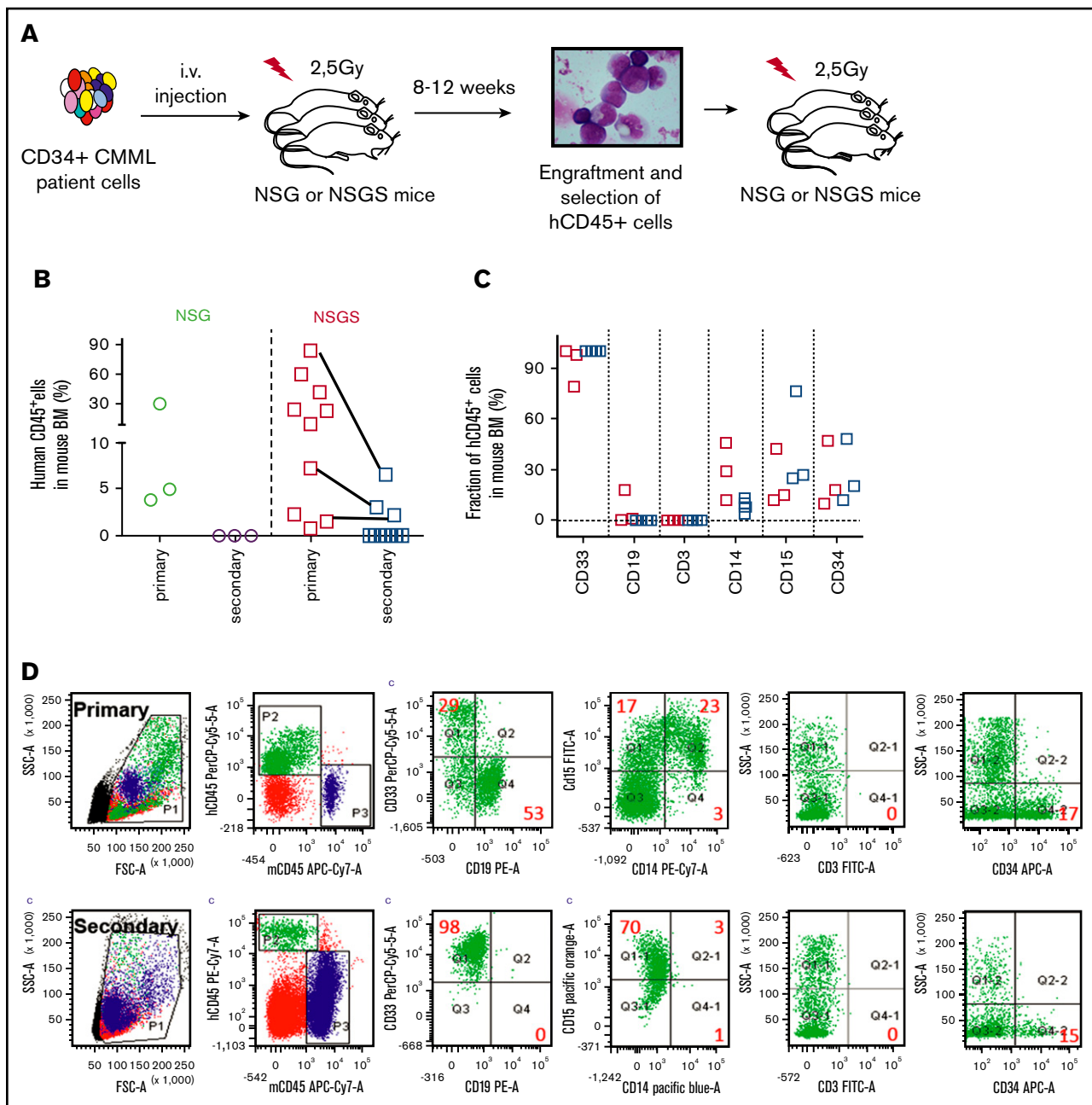


**Figure 4. Secondary engraftment of CMML cells.** (A) General experimental procedure for engraftment. Human cells were sorted from BM samples collected from primary mice and injected to secondary NSG or NSGS mice. (B) Comparison of secondary transplantation of NSG (green and purple circles) and NSGS (red and blue squares) mice. Multiparametric flow cytometry was used to identify the immunophenotype of human cells (C) and representative dot plots of flow cytometry of BM cells from primary and secondary recipient NSGS mice xenografted from S788 (D).

1 mL of PBS, cells were pelleted, and the supernatant was collected. Spleen and a half lobe of liver after weighing were crushed in 0.5 mL and 1 mL PBS, respectively. Supernatants were collected after centrifugation. All samples were stored at  $-80^{\circ}\text{C}$  until use. Human SCF levels were evaluated by a Quantikine enzyme-linked immunosorbent assay kit from R&D System (Europe Ltd., United Kingdom). Human GM-CSF and IL-3 were evaluated by U-PLEX Biomarker Group 1 (hu) Assays (MSD, Rockville, MD). All concentrations that registered below the lower limit of detection for the analyte were considered as 0. Cytokine concentration in BM was calculated as

follows: detected concentration (pg/mL)  $\times$  50 because the volume of 1 femur was considered as  $10\ \mu\text{L}$ . The cytokine concentration in spleen and liver were calculated as follows: detected concentration (pg/mL)  $\times$  0.5 and 1, respectively, then divided by their weight. Data are presented by picogram per milligram of organ weight.

### Statistics

Data obtained from repeated experiments are reported as the mean  $\pm$  standard deviation. Differences in the distribution of continuous variables between categories were analyzed by Mann-Whitney

U test and Student *t* test. The BiostaTGV (<http://marne.u707.jussieu.fr/biostatgv>) statistical package was used for all these calculations. In all evaluations, differences were considered as significant if the *P* value was  $<.05$ .

## Results

Sublethally irradiated mice were injected IV with CD34<sup>+</sup> cells sorted from BM or PB samples (supplemental Table 1) collected from 16 CMML patients (Figure 1A; supplemental Tables 2 and 3). Human CD45<sup>+</sup> cells were detected by flow cytometry 4 to 16 weeks after transplantation in mouse blood and BM with a reliable detection of CD45<sup>+</sup> cells above background fluorescence of 1% as illustrated in Figure 1A. Low levels of human CD45<sup>+</sup>CD33<sup>+</sup> myeloid cells were detected in the PB of NSG mice injected with cells from 9/11 (>80%) CMML patients (see 4 examples in Figure 1B). The fraction of human cells subsequently decreased in all cases but 1 in which they slightly expanded, still remaining below 5% of blood cells 14 weeks after transplantation (Figure 1B, right). At euthanization, human CD45<sup>+</sup>CD33<sup>+</sup> cells could be detected in 9 out of 11 cases, ranging from 1% to 31% of total BM cells (Figure 1C,F). In contrast, the fraction of human CD45<sup>+</sup>CD33<sup>+</sup> myeloid cells detected in the PB of NSGS mice injected with cells from 8 CMML patients always increased over time, up to 30% of cells (see two examples in Figure 1D). With these percentages of human cells, white blood cell and monocyte counts were not significantly increased in transplanted compared with noninjected mice, even in NSGS strain (supplemental Figure 1A-F), and mice remained healthy over the course of the study, even though a discrete splenomegaly, with higher spleen weight in NSGS compared with NSG mice, could be observed at euthanization (supplemental Figure 1G-I). Human CD45<sup>+</sup>CD33<sup>+</sup> cells were detected in the BM of every mouse, ranging from 5.6% to 95.0% of total BM cells (Figure 1E-F). In 3 cases, split experiments were performed by simultaneous injection of CD34<sup>+</sup> cells into NSG and NSGS mice. The fraction of hCD45<sup>+</sup>CD33<sup>+</sup> cells was always higher in the PB (eg, S994 in Figure 1D) and in the BM (Figure 1F) of NSGS compared with NSG mice. BM was the major site of human CD45<sup>+</sup>CD33<sup>+</sup> myeloid cell infiltration, with a more limited number of human cells detected in the PB and the spleen of NSG and NSGS mice (Figure 2A). Histopathological analysis of the BM, spleen, and liver confirmed a significantly higher fraction of human CD45<sup>+</sup> cells in NSGS compared with NSG tissues (Figure 2B), which was consistent with a high concentration of the 3 human cytokines in the mouse plasma and in these 3 mouse tissues (Figure 2C). We then assessed the phenotype of BM-engrafted cells using multiparametric flow cytometry analysis as depicted in Figure 3A. Interestingly, cells with myeloid cell surface markers (CD33, CD15, and CD14) represented the majority of human cells, and a smaller fraction expressed CD19 and CD3, indicating the preferred engraftment and expansion of myeloid cells, even though a small fraction of cells expressing CD34<sup>+</sup> was still detected (Figure 3A-B). There was no significant difference in the phenotype of cells that developed in NSG and NSGS. Of note, a fraction of hCD45<sup>+</sup>CD33<sup>+</sup> cells did not express any of the studied markers. Altogether, these results suggest that injected cells differentiate mostly into myeloid cells in the mouse environment. Accordingly, cytological analyses of human cells sorted from the 2 mouse strains showed predominantly monocytes (including dystrophic monocytes, promonocytes, and monoblasts) and myeloblasts (Figure 3C).

We also investigated the relationship between the level of engraftment and various clinical characteristics of the CMML. The median white blood cell count was very similar for cases with high or low engraftment, and no statistically significant difference could be detected. Similarly, the hemoglobin, platelets, and age of the patients could not be used as predictive markers of engraftment levels of the patients (not shown). We did not find any correlation between engraftment levels and the mutational status or the disease prognostic score (supplemental Table 2).<sup>14</sup> In 4 cases, the main variants detected in patient sorted monocytes could be analyzed in human cells expanded in NSGS mice (supplemental Table 4), showing a good correlation between variant allele frequencies (VAFs) of gene mutations measured in sorted cells before and after engraftment (Figure 3D). Of note, some clonal sweeps were detected; for example, the VAF of an *NRAS* gene mutation detected in S892 dramatically decreased in engrafted cells, whereas other mutants remained stable and a *KRAS* variant that had not been detected before engraftment was present in 27% of engrafted cells (supplemental Table 4). In 3 other cases, the VAF of the detected mutations had not been measured in patient cells before engraftment but were similar in 2 independently engrafted mice (supplemental Table 5).

We subsequently performed secondary transplantations (supplemental Table 1; Figure 4A). None of 3 samples, of which 2 were collected from engrafted NSG mice (P509 and P811) and 1 from engrafted NSGS mice (P994) secondarily engrafted into NSG mice. Three of 10 samples engrafted primarily in NSG (*N* = 3) or NSGS (*N* = 7) mice successfully engrafted in secondary NSGS recipients with 2% (*n* = 2), 3% (*n* = 2), and 9% (*n* = 2) of human cells in the BM for S752, S892, and S788, respectively (supplemental Table 1; Figure 4B). Using multiparametric flow cytometry analysis depicted in Figure 4D, we noticed that all the secondary engrafted CD45<sup>+</sup> cells expressed CD33, whereas 20% to 80% expressed CD15 and none expressed CD14 (Figure 4C-D). This observation suggests that secondary transplant does not faithfully reproduce CMML as granulocytic differentiation has become prominent. NGS analysis of human BM cells sorted from a secondary engrafted mouse (supplemental Table 5; patient #788) identified the mutation detected in patient sorted monocytes, indicating expansion of cells from the leukemic clone.

## Discussion

In this study, we observed that 15 out of 16 CMML samples successfully engrafted in either NSG or NSGS mice or both. Compared with NSG mice, NSGS mice demonstrated a superior overall engraftment efficacy (96% against 50%; supplemental Table 1). Paired analysis with split samples showed that human myeloid cell expansion in BM and extramedullary organs was greatly enhanced in NSGS compared with NSG mice. In addition, this model mostly preserved the molecular characteristics of the primary disease. Previous studies demonstrated that GM-CSF produced by either autocrine or paracrine mechanisms was a major growth determinant for CMML patient cells because of hypersensitivity of CMML patient myeloid progenitors to the cytokine. This hypersensitivity was shown to be independent of any change in receptor density at the cell surface and was highly specific (ie, CMML cells were not hypersensitive to IL-3 or G-CSF).<sup>4</sup> The improvement of CMML cell engraftment in mice expressing human GM-CSF, IL3, and SCF may be related mostly to GM-CSF, although we cannot



formally exclude a role for SCF and IL3. The use of single separated knockin mice would provide a more precise answer on the impact of each cytokine on engraftment, as demonstrated previously.<sup>10-12</sup>

Although primary transplantation was effective for most patient samples, secondary transplantation was observed for a limited number of cases. This low efficacy may be the consequence of the expansion of GM-CSF hypersensitive progenitors while engraftment of leukemic stem cells may remain limited in these conditions. High human cytokine concentrations could also create an inflammatory environment that compromises human stem cell regeneration.<sup>16,17</sup>

Altogether, we observed a successful primary engraftment of CMML samples in either NSG or NSGS mice or both indicating that engraftment of primary CMML in immunodeficient mice is feasible, which may help understanding the physiopathology of CMML. However, the difficulties in establishing secondary transplantation underline the need to develop alternative approaches for pre-clinical evaluation of new therapeutic strategies in this disease.

## Acknowledgments

The authors thank all patients and their physicians who participated in the study. The authors are grateful to Cyril Quivron for his helpful assistance in animal experiments, Véronique Saada for her advice in cytology, and Franck Debeurme for his help in clinical data collection.

## References

1. Arber DA, Orazi A, Hasserjian R, et al. The 2016 revision to the World Health Organization classification of myeloid neoplasms and acute leukemia. *Blood*. 2016;127(20):2391-2405.
2. Merlevede J, Droin N, Qin T, et al. Mutation allele burden remains unchanged in chronic myelomonocytic leukaemia responding to hypomethylating agents. *Nat Commun*. 2016;7(7):10767.
3. Patnaik MM, Tefferi A. Chronic myelomonocytic leukemia: 2016 update on diagnosis, risk stratification, and management. *Am J Hematol*. 2016;91(6):631-642.
4. Padron E, Painter JS, Kunigal S, et al. GM-CSF-dependent pSTAT5 sensitivity is a feature with therapeutic potential in chronic myelomonocytic leukemia. *Blood*. 2013;121(25):5068-5077.
5. Padron E, Dezern A, Andrade-Campos M, et al; Myelodysplastic Syndrome Clinical Research Consortium. A multi-institution phase I trial of ruxolitinib in patients with chronic myelomonocytic leukemia (CMML). *Clin Cancer Res*. 2016;22(15):3746-3754.
6. Ball M, List AF, Padron E. When clinical heterogeneity exceeds genetic heterogeneity: thinking outside the genomic box in chronic myelomonocytic leukemia. *Blood*. 2016;128(20):2381-2387.
7. Ramshaw HS, Bardy PG, Lee MA, Lopez AF. Chronic myelomonocytic leukemia requires granulocyte-macrophage colony-stimulating factor for growth in vitro and in vivo. *Exp Hematol*. 2002;30(10):1124-1131.
8. Shultz LD, Ishikawa F, Greiner DL. Humanized mice in translational biomedical research. *Nat Rev Immunol*. 2007;7(2):118-130.
9. Billerbeck E, Barry WT, Mu K, Dorner M, Rice CM, Ploss A. Development of human CD4+FoxP3+ regulatory T cells in human stem cell factor-, granulocyte-macrophage colony-stimulating factor-, and interleukin-3-expressing NOD-SCID IL2Rγ(null) humanized mice. *Blood*. 2011;117(11):3076-3086.
10. Saito Y, Ellegast JM, Rafiei A, et al. Peripheral blood CD34+ cells efficiently engraft human cytokine knock-in mice. *Blood*. 2016;128(14):1829-1833.
11. Rauch PJ, Ellegast JM, Widmer CC, et al. MPL expression on AML blasts predicts peripheral blood neutropenia and thrombocytopenia. *Blood*. 2016;128(18):2253-2257.
12. Ellegast JM, Rauch PJ, Kovtonyuk LV, et al. inv(16) and NPM1mut AMLs engraft human cytokine knock-in mice. *Blood*. 2016;128(17):2130-2134.
13. Such E, Cervera J, Costa D, et al. Cytogenetic risk stratification in chronic myelomonocytic leukemia. *Haematologica*. 2011;96(3):375-383.
14. Itzykson R, Kosmider O, Renneville A, et al. Prognostic score including gene mutations in chronic myelomonocytic leukemia. *J Clin Oncol*. 2013;31(19):2428-2436.
15. Zhang Y, Patel S, Abdelouahab H, et al. CXCR4 inhibitors selectively eliminate CXCR4-expressing human acute myeloid leukemia cells in NOG mouse model. *Cell Death Dis*. 2012;3(10):e396.
16. Swirski FK, Nahrendorf M. Inflammation: old, caffeinated, and healthy. *Nat Rev Cardiol*. 2017;14(4):194-196.
17. Nicolini FE, Cashman JD, Hogge DE, Humphries RK, Eaves CJ. NOD/SCID mice engineered to express human IL-3, GM-CSF and Steel factor constitutively mobilize engrafted human progenitors and compromise human stem cell regeneration. *Leukemia*. 2004;18(2):341-347.

This work was supported by grants from INSERM, the Fondation Gustave Roussy (F.L.), Fondation de France (F.L.), Association Laurette Fugain (F.L.), and Cancéropole, Ile de France (F.L.). Y.Z. was supported by a postdoctoral fellowship from the Institut du Cancer. L.H. was supported by a fellowship from China Scholarship Council.

## Authorship

Contribution: Y.Z. designed and performed experiments, analyzed data, and wrote the manuscript; D.S.-B. performed multiparametric flow cytometry; N.D. and M.K.D. performed gene sequencing; L.H., C.J., and M.M. performed experiments; C.W. provided the follow-up information on patients; P.G. performed statistical analysis; V.L. discussed the results; E.S. discussed the results and wrote the manuscript; and F.L. directed the study, discussed the results, and wrote the manuscript.

Conflict-of-interest disclosure: The authors declare no competing financial interests.

ORCID profiles: P.G., 0000-0001-6151-4580; F.L., 0000-0002-4247-5421.

Correspondence: Fawzia Louache, Inserm U1170, Pavillon de Recherche N°1, Gustave Roussy, 114 rue Edouard Vaillant, 94805 Villejuif, France; e-mail: fawzia.louache@gustaveroussy.fr.